Journal of the European Ceramic Society 36 (2016) 3293–3302

Contents lists available at www.sciencedirect.com

Journal of the European Ceramic Society

journal homepage: www.elsevier.com/locate/jeurceramsoc

Oxidation behaviour of SiC/SiC ceramic matrix composites in air

Nasrin Al Nasiri*, Niranjan Patra, Na Ni, Daniel D. Jayaseelan, William E. Lee

Centre for Advanced Structural Ceramics, Department of Materials, Imperial College London, South Kensington Campus, London SW7 2BP, United Kingdom

ARTICLE INFO

Article history:
Received 14 March 2016
Received in revised form 25 May 2016
Accepted 30 May 2016
Available online 14 June 2016

Keywords:
Oxidation
SiC/SiC
CMC
BN coating and activation energy

ABSTRACT

Oxidation of silicon melt infiltrated SiC/SiC ceramic matrix composites (CMC) was studied in air at 1200–1400 °C for 1, 5, 24 and 48 h. Weight gain and oxide layer thickness measurements revealed the oxidation follows parabolic reaction kinetics with increase in temperature and time. XRD showed the extent of oxide layer (SiO_2) formation was greatest after 48 h at 1400 °C: an observation confirmed by X-ray photoelectron spectroscopy (XPS), energy dispersive spectroscopy (EDS) and transmission electron microscopy (TEM) analyses. Oxide layer thickness varied from 1 μm after 48 h at 1200 °C to 8 μm after 48 h at 1400 °C. Oxidation of SiC/SiC composites is both temperature and time dependent with an activation energy of 619 kJ mol^{-1}. BN coatings around SiC fibres showed good resistance to oxidation even after 48 h at 1400 °C.

© 2016 Elsevier Ltd. All rights reserved.

1. Introduction

The need to increase the cycle efficiency and reduce noise and NO_x emissions from jet engine turbines has promoted development of ceramic matrix composites (CMC) such as silicon carbide fibre-reinforced silicon carbide (SiC-SiC) [1–3]. Use of CMCs will lead to a significant improvement in fuel consumption and thrust-to-weight ratio compared to metal alloys. In addition, the low density of CMCs allows weight savings of up to 30% compared to Ni-based super alloys equating to about 1000 kg/engine thus leading to vastly improved fuel consumption [4]. At high temperature >900 °C, SiC may undergo either active or passive oxidation [5]. At low oxygen pressures (<1 atm), active oxidation occurs due to the formation of volatile products as follows:

$$SiC(s) + 2SiO_2(s) \rightarrow 3SiO(g) + CO(g) \quad (1)$$

$$SiC(s) + O_2(g) \rightarrow SiO(g) + CO(g) \quad (2)$$

During passive oxidation a protective film of SiO_2 is formed on the surface according to:

$$SiC(s) + \frac{3}{2}O_2(g) \rightarrow SiO_2(s) + CO(g) \quad (3)$$

$$SiC(s) + 2O_2(g) \rightarrow SiO_2(s) + CO_2(g) \quad (4)$$

Castello and Tressler [6] studied the oxidation behaviour of sintered SiC and chemical vapour deposition (CVD) SiC at 1200–1500 °C in dry oxygen. They observed a parabolic behaviour and suggested that oxidation is controlled by permeation of oxygen ions through the growing oxide film. However, the oxidation rates of CVD SiC were higher than those of sintered SiC due to the presence of free silicon. Schiroky [7] studied oxidation behaviour of CVD SiC at 1200–1800 °C. At >1500 °C, growth of uniform films of amorphous silica was observed and with bubble formation between 1700 and 1800 °C due to the high CO pressure at SiC-SiO_2 interfaces. Oxidation of CVD SiC was also investigated by Narushima et al. [8] at 1550–1700 °C. They observed that the parabolic oxidation behaviour of CVD SiC consists of stage I and stage II as a result of a change in diffusion rate of oxygen in the SiO_2 film due to crystallization from amorphous silica to β-cristobalite. However, in both stages, the parabolic rate constant (k) depends on the oxygen partial pressure meaning that the rate controlling process for oxidation is diffusion of the oxygen ions in the SiO_2 film. They obtained activation energies of 345 and 387 kJ mol^{-1} for stage I and stage II respectively at 1550–1700 °C in reasonable agreement with values obtained by Sucov (420 kJ mol^{-1}) at 700–1200 °C [9].

Only a few reports on the oxidation of SiC/SiC composites are available in the literature. Kleykamp et al. [10] were the first to investigate the influence of carbon-coated SiC fibre reinforcement on the oxidation behaviour of SiC at 550–1520 °C in air. They observed that at 870–985 °C, the amorphous SiO_2 transforms to tetragonal cristobalite and oxidation kinetics follow a quadratic rate law above 1000 °C. Moreover, no apparent improvement in corrosion resistance of SiC fibre-reinforced SiC compared to dense monolithic SiC was observed due to the high porosity (10 vol%) of the SiC matrix and the free carbon in the interlayers that is burnt out over the lower temperature range. Sheldon et al. [11]

* Corresponding author.
E-mail address: n.al-nasiri10@imperial.ac.uk (N.A. Nasiri).

http://dx.doi.org/10.1016/j.jeurceramsoc.2016.05.051
0955-2219/© 2016 Elsevier Ltd. All rights reserved.

studied the oxidation behaviour of boron nitride (BN) coated SiC fibres in CMC at 1000–1450 °C. They suggested that oxidation of this material undergoes three different stages, where stage I represents oxidation of SiC to form SiO_2 and solid carbon according to:

$$SiC(s) + O_2(g) \rightarrow SiO_2(s) + C(s) \quad (5)$$

After all the available SiC has oxidised, stage II is active where the oxidation of solid carbon takes place to produce CO, where stage III corresponds to oxidation of the BN coating as follows:

$$2BN(s) + \frac{3}{2}O_2(g) \rightarrow B_2O_3(l) + N_2(g) \quad (6)$$

They observed that formation of SiO_2 takes place before formation of B_2O_3 meaning that BN-coated SiC fibres will not necessarily lead to formation of a low melting oxide phase such as borosilicate glass, in agreement with Jacobson et al. [12].

Based on the above discussion, this work focuses on the oxidation behaviour and kinetics of BN-coated SiC-reinforced SiC composites at 1200–1400 °C in dry air for different periods of time. The main aim was to investigate the influence of several parameters (temperature and time) on the oxidation behaviour of SiC/SiC composites and to characterise formation of SiO_2 as a function of time.

2. Experimental methods

BN coated SiC/SiC composites were manufactured through chemical vapour infiltration (CVI) and slurry infiltration of SiC and then impregnated with liquid silicon. The SiC matrix and fibres are bonded together via a boron nitride fibre coating on the fibres, details are given elsewhere [13]. The samples were cut to 10 × 10 × 4 mm, then cleaned with acetone in an ultrasonic bath and dried in a vacuum oven for 24 h prior to testing. Oxidation experiments were conducted at 1200–1400 °C for 1, 5, 24 and 48 h in a lift furnace under static air and samples were quenched in air after each hold. Samples were placed on high purity >99.99% alumina boats (Almath crucibles, Newmarket, UK) in contact with their two edges to minimize the contact area between samples and crucible and then placed inside a chamber lift furnace (Lenton, Hope, UK) at a heating rate of 10 °C min^{-1}. The weight and dimensions of all samples were recorded before and after the experiment with precision of ±0.001 g and ±0.01 mm respectively.

Oxidation kinetics were analysed using a parabolic power law as follows [14]:

$$\left(\frac{\Delta w}{A}\right) = \sqrt{k.t} \quad (7)$$

where, Δw is the weight change before and after oxidation, A is the total surface area, k is the parabolic rate constant and t is the oxidation time. The activation energy (E) needed for oxidation was determined according to the Arrhenius equation [5]:

$$k = A.e^{(-E/RT)} \quad (8)$$

where, A is a constant, R is the gas constant and T is absolute temperature.

Samples before and after oxidation were characterised using XRD (Bruker instrument, Coventry, UK). XRD measurements were carried out in 2θ range of 10–80°. Phases were identified using Xpert High Score Plus software utilising the ICDD (International Centre for Diffraction Data) database.

Samples oxidised at 1400 °C for 1, 5, 24 and 48 h were analysed using XPS (K-Alpha, Thermo scientific, Warrington, UK) to determine the nature of the oxide layer through their binding energies. XPS measurements were conducted using Mg X-rays of 1253.6 eV. Photoelectrons from Si-2*p*, C–1s and O–1s core levels were collected using a hemispherical analyser with 50 eV pass energy, a 200 ms integration time and 0.1 eV steps. The analysis was performed using CasaXPS software. Shirley or two point linear background subtractions were employed depending on background shape. Scofield cross-sections were used as relative sensitivity factors in the calculation of the atomic percentages with relative sensitivity factor (RSF) of C 1s = 1.000. Peaks were fitted using GL(30) lineshapes; a combination of a Gaussian (70%) and Lorentzian (30%). All XPS spectra were charge corrected by referencing the fitted contribution of C—C graphitic like carbon in the C 1s signal to 284.6 eV.

Microstructures were examined in back scattered and secondary electron imaging (BSI and SEI, respectively) modes using a scanning electron microscope (SEM) JEOL (JSM 6010LA, Tokyo, Japan) also equipped with an energy dispersive spectroscopy (EDS) JOEL silicon drift detector (SDD) with ultra-thin window (UTW). Samples were mounted in epoxy resin and cut at 90 ° using diamond blade and polished to 1 μm and 0.06 μm suspensions of diamond and silica colloidal respectively. Samples were cleaned in an ultrasound acetone bath for 1 min to remove any contamination during polishing. Prior to SEM, samples were coated in gold to avoid electrical charging. The average oxide layer thickness (±0.5 μm) was obtained based on 200 points of both oxide faces from SEM micrographs using Image-J software.

The crystalline structures and chemistry of the as-received and oxidised samples of SiC/SiC CMC were characterised by Transmission Electron Microscopy (TEM). Cross-sectional TEM samples were prepared by focused ion beam (FIB) milling (Helios NanoLab 600). TEM bright field and Scanning Transmission Electron Microscopy (STEM) imaging was carried out on a JEOL (JSM 2100F, Tokyo, Japan)

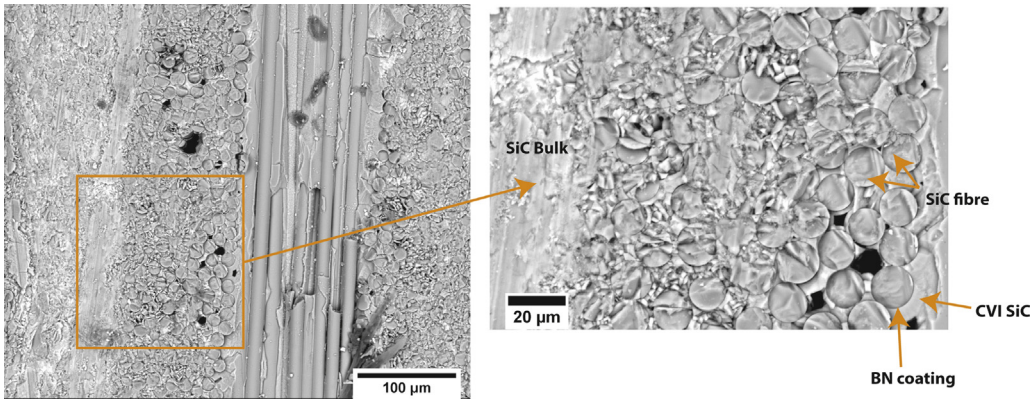

Fig. 1. SEI microstructure of BN coated SiC/SiC composites as received from supplier revealing the SiC bulk and fibres.

operated at 200 kV. EDS in the STEM was done using INCA software (Oxford instrument, Abingdon, UK) and electron diffraction pattern (DP) capture using a Gatan digital camera (Gatan, Abingdon, UK).

Electron Energy Loss Spectroscopy (EELS), work was carried out in STEM mode on a FEI Titan 80–300 S/TEM operated at 300 kV, equipped with a monochromator and a Cs aberration image corrector. The incident angle α and collection angle β for EELS acquisitions were ~10 and ~14 mrad, respectively. Hydrocarbon contamination can originate from sample handling and preparation processes and is common for TEM specimens. A plasma cleaning step before the TEM experiments is normally applied to remove it, however this could not be used for the current samples due to formation of water molecules during the plasma cleaning process and the sensitivity of the coating to moisture. The main issue with hydrocarbon contamination for STEM-EELS is that the mobile hydrocarbon molecules move towards the electron beam and are polymerized by the

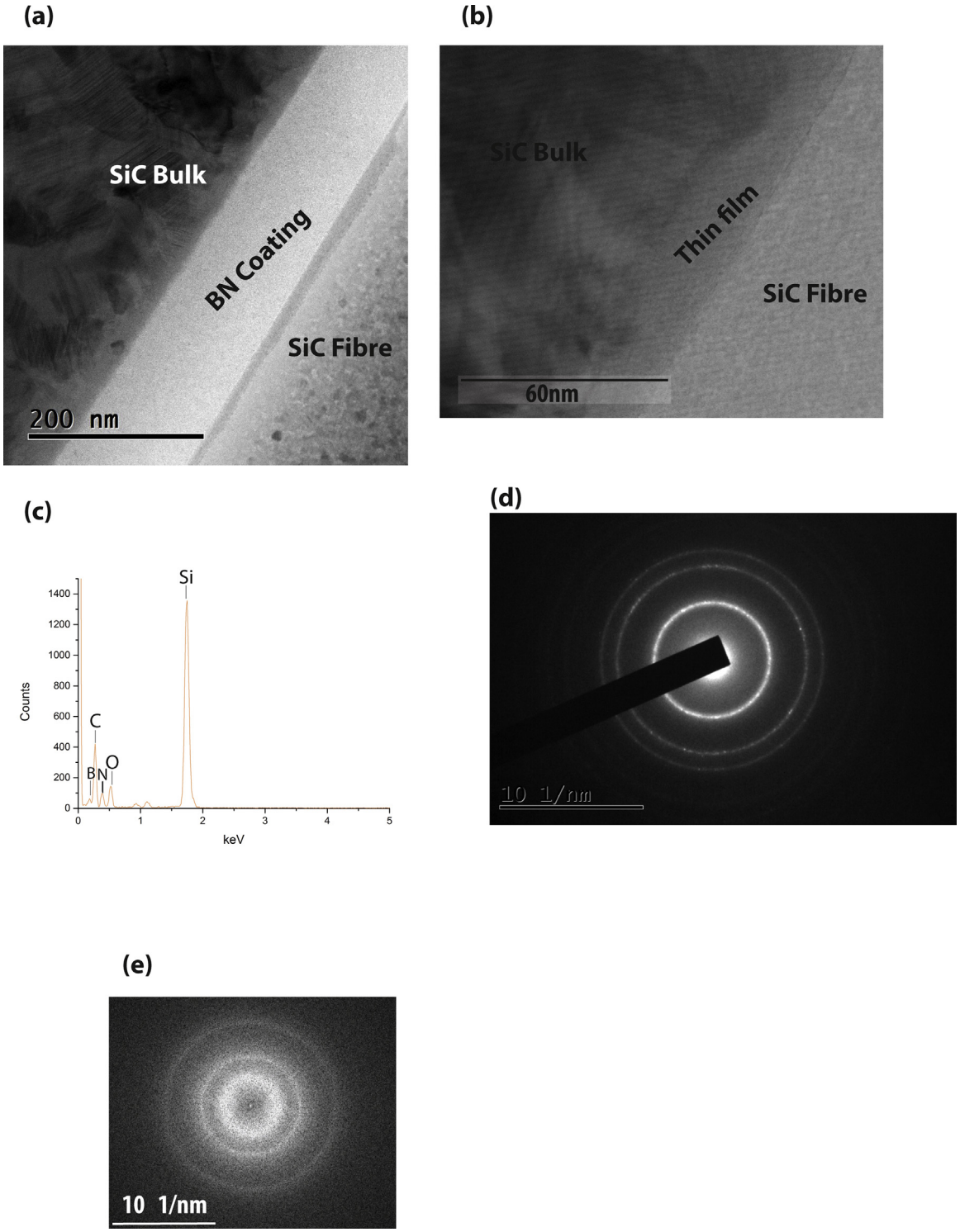

Fig. 2. High magnification BF TEM image of: (a, b) SiC bulk and fibre with BN coating interphase before oxidation, (c) EDS of BN coating, (d) DP of SiC fibre and (e) DP of BN coating.

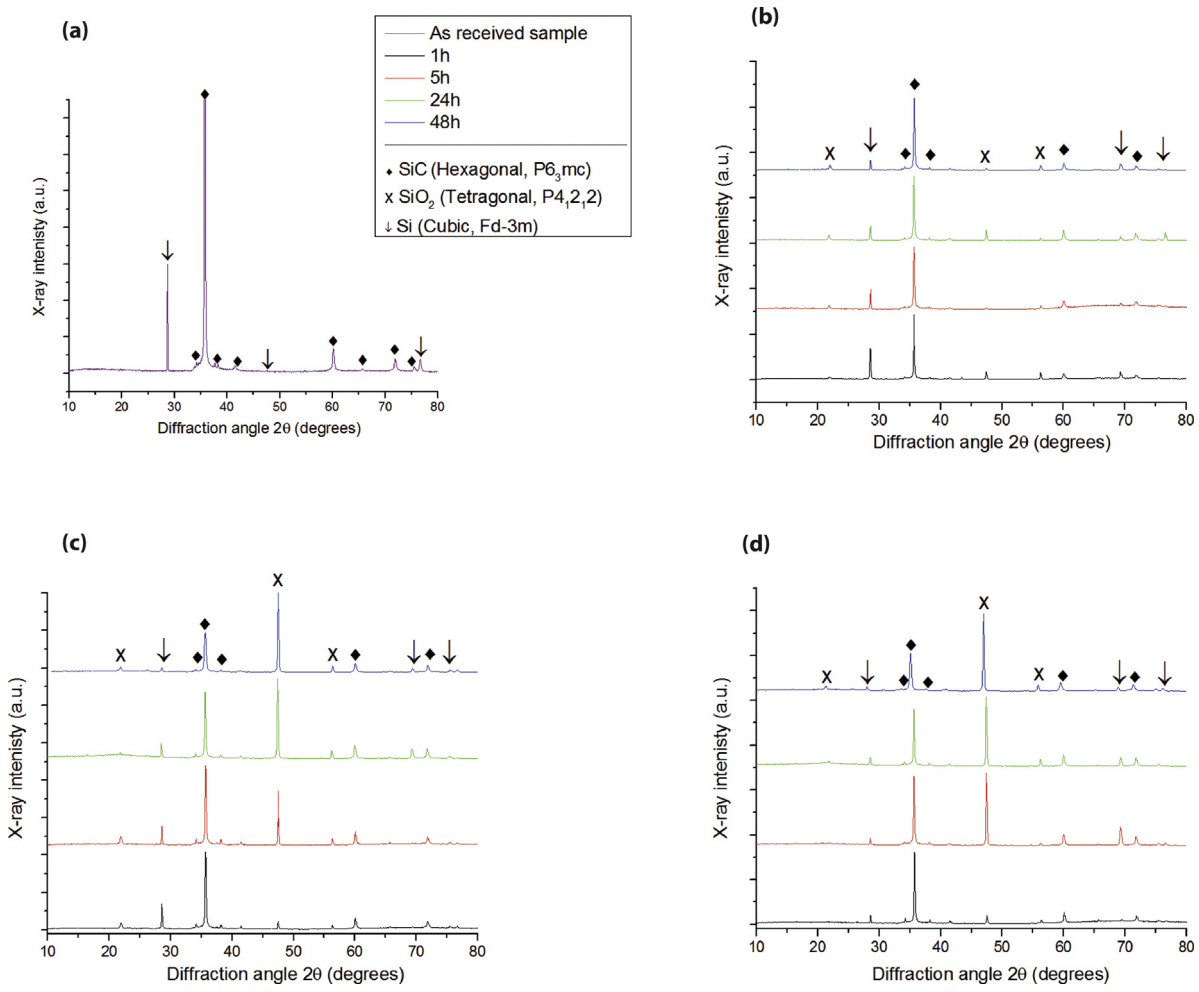

Fig. 3. XRD of BN coated SiC/SiC for: (a) as received sample, (b) oxidised at 1200 °C, (c) oxidised at 1300 °C and (d) oxidised at 1400 °C for 1, 5, 24 and 48 h.

electrons, leading to a continuous increase in the local specimen thickness at the probe position, which makes EELS measurement impossible. To tackle the problem, a beam shower procedure inside the TEM [15] was carried out, which successfully reduced the mobility of the hydrocarbon so that during the spectrum acquisition continuous build-up of hydrocarbon under the STEM probe was avoided. In this condition, the relative specimen thickness (thickness over electron inelastic mean free path, t/λ) was checked to be below ~0.4 for all EELS analysis, sufficiently thin to enable valid analysis of the interested elements (B, N and O) without interference from carbon.

3. Results and discussion

SEIs of as-received BN-coated SiC/SiC (Fig. 1) revealed the SiC matrix, fibres and BN coating on the SiC fibres. A bright-field TEM image of a region in the as-received sample is shown in Fig. 2(a). A typical interface between the SiC fibre and SiC matrix shows about 100 nm thick BN coating on the fibre. Fig. 2(b) shows typical SiC matrix-BN coating-SiC fibre interfaces. On both sides of the BN-coating, a thin (about 10 nm) film is observed (Fig. 2(b)). EDS analysis of this thin film (Fig. 2(c)) reveals the main elements of the BN-coating with some oxygen contamination due to FIB milling while the peaks of Si and C are from SiC neighbours. Electron diffraction patterns (Fig. 2d and e), indicate the coatings are largely amorphous, while the SiC fibres are polycrystalline.

XRD of samples before and after oxidation at 1200–1400 °C for 1, 5, 24 and 48 h is shown in Fig. 3. Before oxidation (Fig. 3a), XRD reveals only 6H-SiC and silicon, where the main silicon carbide and silicon peaks are at 2θ of 35.7° and 28.5° respectively. After oxidation at 1200 °C, the intensity of the main silicon peak decreases with an increase in the oxidation time, where it is lowest after 48 h oxidation at 1400 °C. On the other hand, the opposite is observed for formation of the oxide layer where the most intense SiO_2 peak (2θ of 48.8°) is highest after 48 h at 1400 °C. It is also observed that oxidation of SiC takes place at all tested temperatures, however the oxidation is greater after holds at 1300–1400 °C as indicated by the decline of the main SiC peak at 2θ of 35.7°. After oxidation at 1200 °C, the SiC peaks did not decrease with increase in oxidation time, whereas the Si peaks decrease with an increase in oxidation time. This suggests that oxidation of Si is predominant over the oxidation of SiC around this temperature. However, after oxidation at 1300 °C, the SiC peaks started to decrease with an increase in the oxidation time, which suggests that the oxidation of SiC is dominant after 1300 °C. Hence, the oxidation of SiC/SiC satisfies Eq. 5 where silicon and SiC react with oxygen to form SiO_2 [11].

There was no change in the morphology of the BN coating after 48 h oxidation at 1400 °C (Fig. 4(a) and (b)) compared to before oxidation (Fig. 2(a) and (e)). EELS spectra from the BN coating before and after oxidation are very similar (Fig. 4c), indicating little change in the composition of the coating. B–K and N–K edges can be clearly seen with a very low intensity O–K edge, which could come from a slight surface oxidation of the thin TEM specimen.

Table 1
Oxidation kinetics in terms of mass gain and oxide layer thickness of BN coated SiC/SiC at 1200–1400 °C.

Oxidation time (h)	1200 °C		1300 °C		1400 °C	
	Δm (mg)	Oxide layer (μm)	Δm (mg)	Oxide layer (μm)	Δm (mg)	Oxide layer (μm)
1	0.1 ± 0.04	0.6 ± 0.09	0.15 ± 0.06	0.9 ± 0.1	1.0 ± 0.4	1.8 ± 0.4
5	0.15 ± 0.07	0.8 ± 0.1	0.4 ± 0.15	1.2 ± 0.2	2.3 ± 0.8	3.4 ± 0.7
24	0.2 ± 0.1	0.9 ± 0.2	0.7 ± 0.04	2.6 ± 0.6	5.8 ± 0.7	6.1 ± 0.9
48	0.4 ± 0.08	1.3 ± 0.4	2.1 ± 0.05	3.6 ± 0.9	7.9 ± 0.7	7.1 ± 1.4

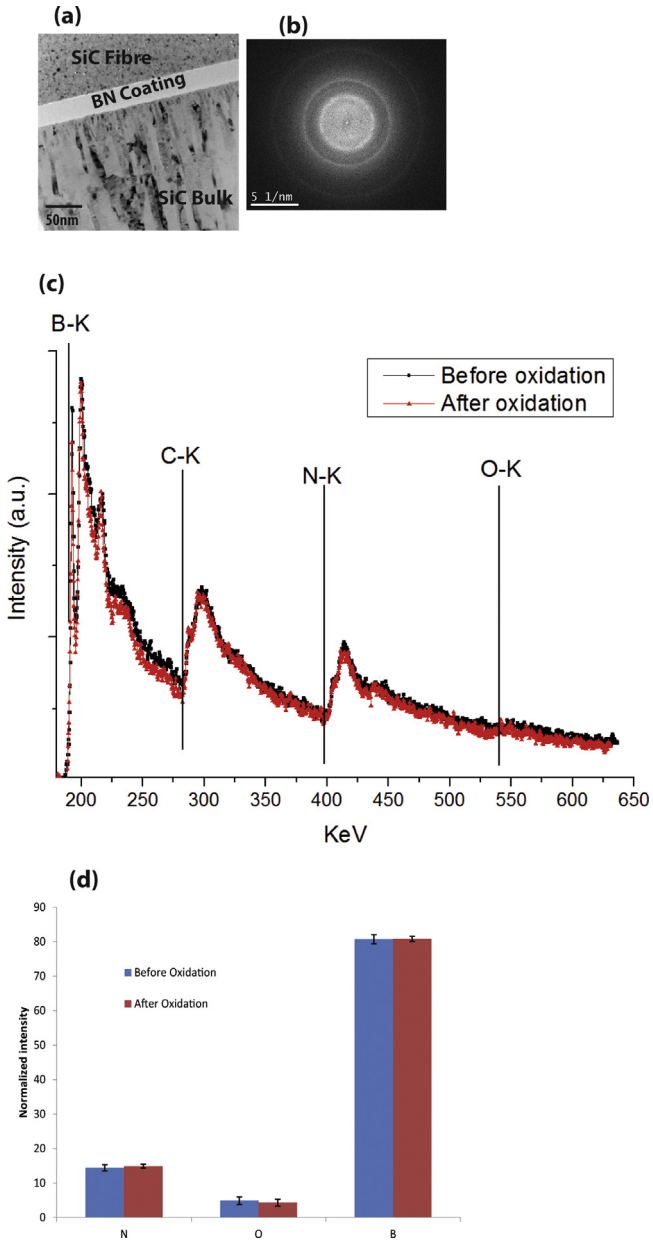

Fig. 4. High magnification BF TEM image of: (a) SiC bulk and fibre with BN coating interphase after oxidation, (b) DP of BN coating, (c) EDS of BN coating before and after oxidation and (d) normalised intensities of B, N and O before and after oxidation.

The C–K edge is present in both samples, and is a result of hydrocarbon contamination at the specimen surface, as mentioned in the experimental section. Although accurate compositional quantification from EELS measurements needs careful calibration with standards, the normalised intensities for B, N and O edges were calculated and averaged from 20 EELS spectra acquired in the coating area. This reveals (Fig. 4d) that the difference between oxidised and non-oxidised samples is within the margin of error indicating that the coating composition is not altered after oxidation.

Oxidation kinetics at 1200, 1300 and 1400 °C are illustrated in Fig. 5, in which mass gain per unit area and oxide layer thickness versus time are presented with best fitting curves according to Eq. (7); these data are summarised in Table 1. Fig. 5 shows clearly that weight is increasing as oxidation temperature and time increasing and is highest after 48 h at 1400 °C. A similar observation is made

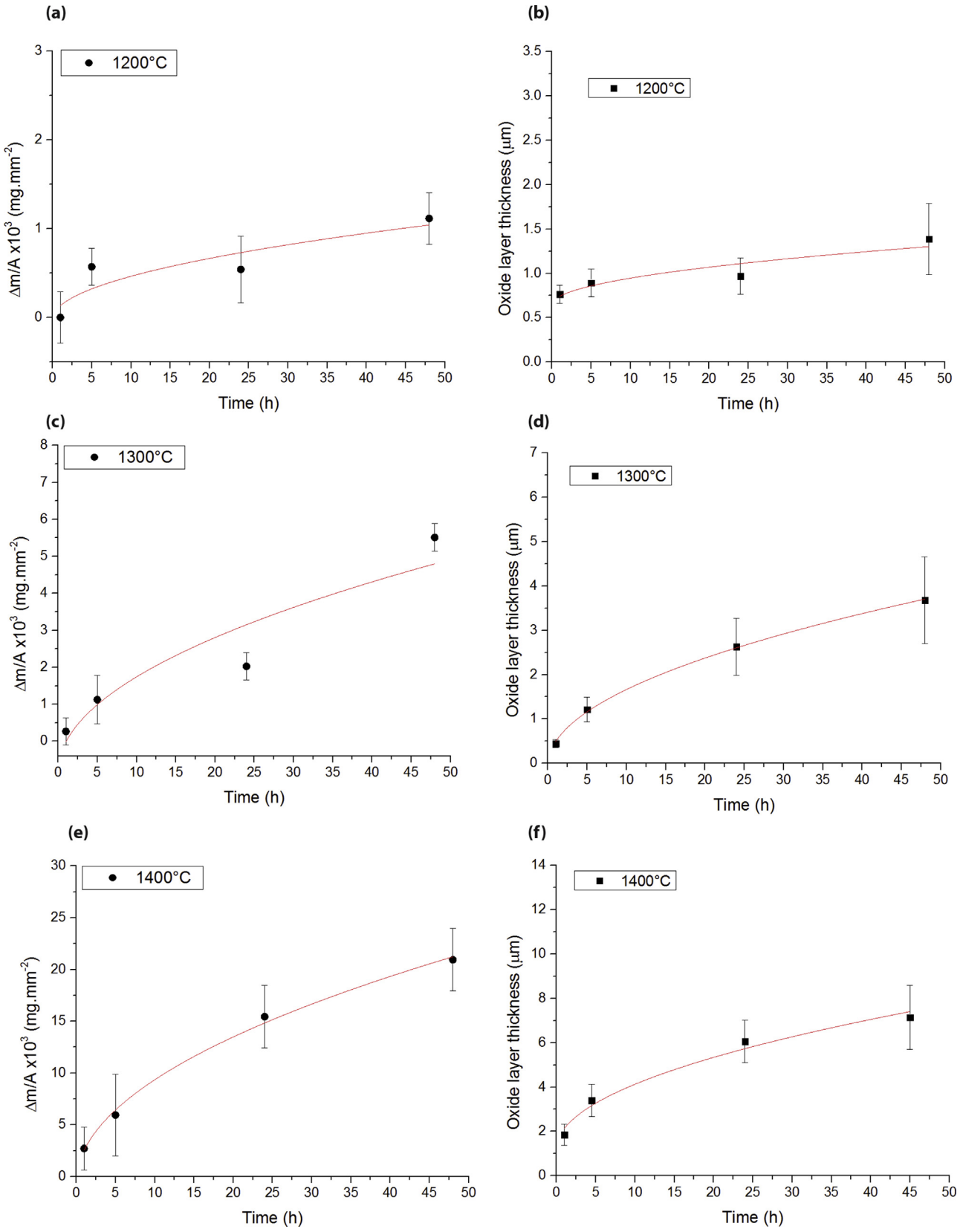

Fig. 5. Mass gain and oxide layer thickness versus time at: (a) and (b) 1200 °C, (c) and (d) 1300 °C and (e) and (f) 1400 °C respectively for BN coated SiC/SiC composites. Best fitting to Eq. (7) is drawn.

Table 3
Activation energy of SiC materials of this study and reported values from the literature.

Material	Temperature range (°C)	Environment	Activation energy (kJ mol^{-1})	Reference
SiC/SiC CMC	1200–1400	Air	619	Present work
HP-SiC	1200–1445	Dry O_2	481	Singhal [5]
HP-SiC	1200–1500	Dry O_2	221	Pultz [20]
CVD SiC	1550–1675	Dry O_2	345	Narushima et al. [8]
CVD SiC	1200–1500	Dry O_2	118	Ogubji and Opila [21]
Sintered SiC	1200–1350	O_2	128	Liu [22]
Sintered SiC	1200–1500	Air	289	Costello and Tressler [6]

Table 2
Summary of oxidation kinetics of BN-coated SiC/SiC at 1200–1400 °C.

	(k),mg^2 mm^{-4} h^{-1}
1200 °C	$2.35 \times 10^{-8} \pm 0.9$
1300 °C	$6.59 \times 10^{-7} \pm 1.3$
1400 °C	$9.95 \times 10^{-6} \pm 2.2$

for the oxide layer thickness which ranges from 1 to 8 μm after 48 h at 1200 and 1400 °C respectively. This parabolic behaviour illustrates that oxidation of SiC/SiC composites is controlled by diffusional mechanisms. It is suggested that the growth of oxide layers on the composites is due to inward diffusion of either oxygen ions or molecules and it depends strongly on temperature and exposed time [16]. Pultz and Hertl [17] suggested that oxidation of SiC is controlled by the CO desorption from the SiC/SiO_2 interface at 1270–1430 °C as upon desorption more sites become available for further oxidation. The parabolic rate constants (k) for the oxidation of BN-coated SiC/SiC composites are given by the slopes of Fig. 5a, c and e and plotted in an Arrhenius plot (Fig. 6). From the slope of Fig. 6 and using Eq. (8), an activation energy (E) for the oxidation of these SiC/SiC composites is ~619 kJ mol^{-1} and listed in Table 2. The activation energy of this study and published values for CMC and monolithic SiC are given in Table 3 revealing a wide variation in the reported values of the activation energy. This may be due to the different materials used in each investigation and the formation of a silica layer in either crystalline or amorphous form. The activation energy obtained in this work is higher than those previously reported indicating that this SiC/SiC composite exhibits better oxidation resistance in air compared to monolithic SiC. This may be due to the formation of a dense and smooth SiO_2 film (Fig. 7). The SiC/SiO_2 interface is observed to be free from pores or defects, which likely makes the diffusion of oxygen through the SiO_2 oxide layer slow conferring higher resistance to oxidation. Another interesting observation is that SiC/SiC CMC of this study shows faster kinetics, but with a steeper activation curve (higher activation energy) compared to CVD SiC (310 kJ mol^{-1}) [18] (Fig. 7). This increase in activation for temperatures >1350 °C is associated with the retention of amorphous SiO_2 and contamination of this scale by small amounts of aluminium from the testing environment. Boron impurity present in the SiC/SiC CMC may be significant where more reaction occurs between boron and SiO_2 layer as temperature increases modifying the glass network for easier oxygen transport.

EDS analysis (Fig. 8) shows that the oxide layer on SiC/SiC composites consists of silicon and oxygen for samples oxidised 48 h at 1200–1400 °C. The oxide layer is smooth, amorphous and continuous on the CMC, with thickness varying with temperature and time. Detailed TEM analysis of the oxide layer on samples oxidised 48 h at 1400 °C is shown in Fig. 9. Fig. 9a shows the location of the TEM samples being milled using FIB and high magnification TEM images of the oxide layer are shown in Fig. 9b and c. EDS analysis (Fig. 9d) reveals only silicon and oxygen consistent with previous analysis

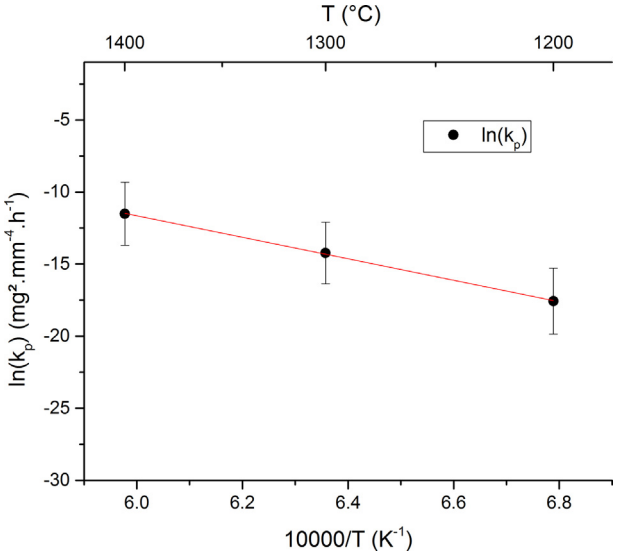

Fig. 6. Parabolic rate constant for the oxidation of BN coated SiC/SiC composites in air at 1200–1400 °C.

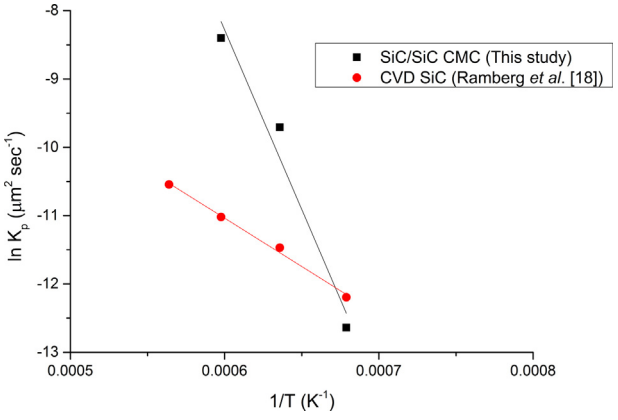

Fig. 7. Comparison of parabolic rate constant for the oxidation of BN coated SiC/SiC composites in air with that of pure CVD SiC.

(Fig. 8(f)). Diffraction pattern analysis (Fig. 9e) shows that the oxide layer is completely amorphous after 48 h oxidation.

XPS analysis of samples oxidised at 1400 °C for 1, 5, 24 and 48 h is given in Fig. 10. The binding energies used to identify the SiC and SiO_2 are according to standards established by Onneby and Pantano [19], where they defined specific energy level of Si (102.5 eV), SiC (99.5–100.1 eV) and SiO_2 (102.5–102.9 eV). After 1 h oxidation at 1400 °C a clear shoulder is seen on the high energy side (102.5 eV) from the SiC substrate (99.5–100.1 eV) confirming the formation

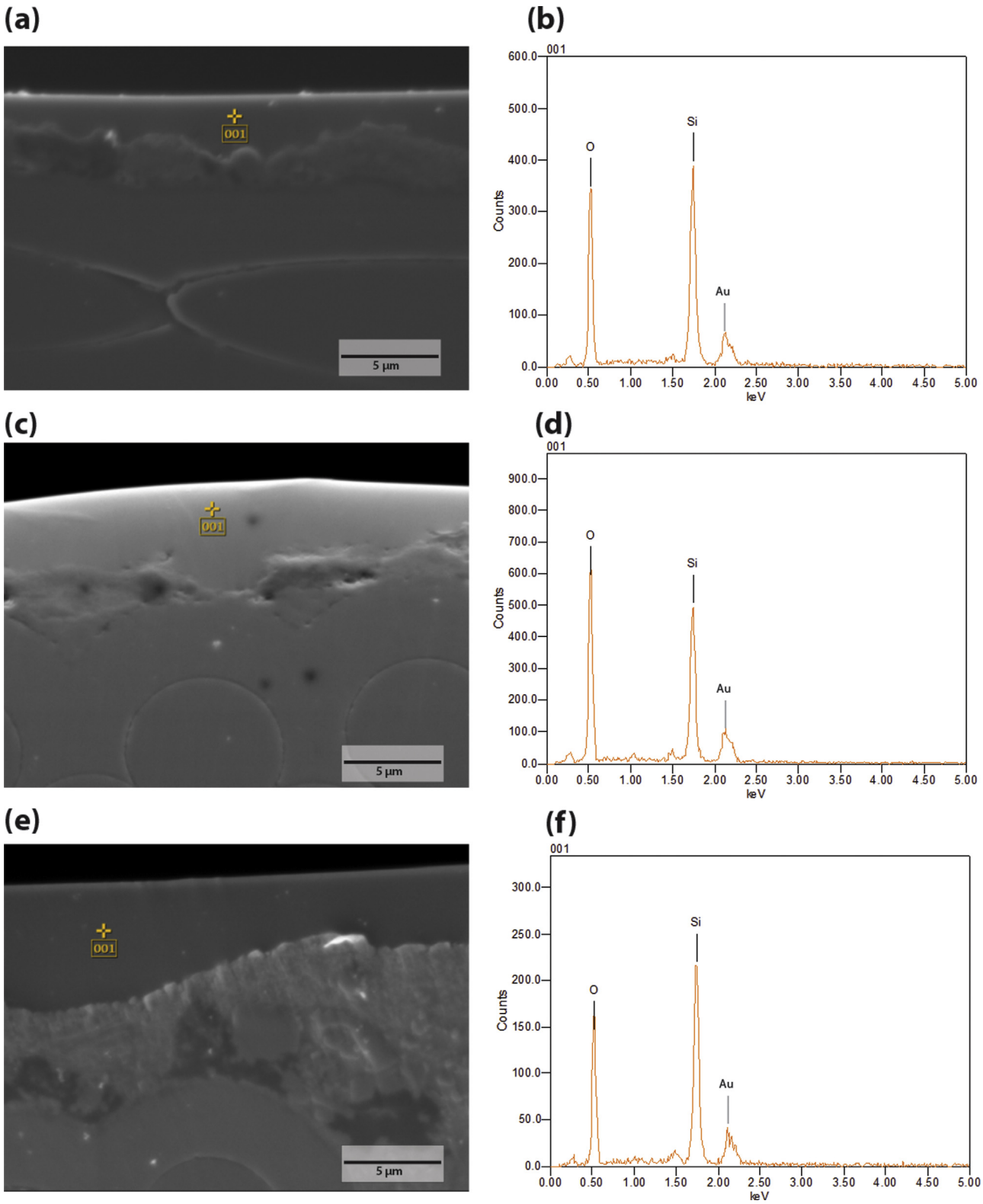

Fig. 8. SEI images and EDX analysis for (a, b) oxidised at 1200 °C, (c, d) oxidised at 1300 °C and (e, f) oxidised at 1400 °C for 48 h.

of an oxidation product of SiO_2 (102.5–102.9 eV). Increasing the oxidation time to 5, 24 and 48 h indicates formation of only SiO_2 around 102.9 eV with no traces of SiC. However, XPS analysis is extremely surface sensitive revealing the formation of species on the surface to 10 nm depth meaning that the oxide overlayers may mask the signal of the SiC substrate.

4. Conclusions

Oxidation of SiC/SiC CMCs at 1200–1400 °C for 1–48 h in air depends on both temperature and time being highest at 1400 °C for 48 h as revealed by weight gain and oxide layer thickness measurements and the oxidation reaction kinetics clearly follow a parabolic

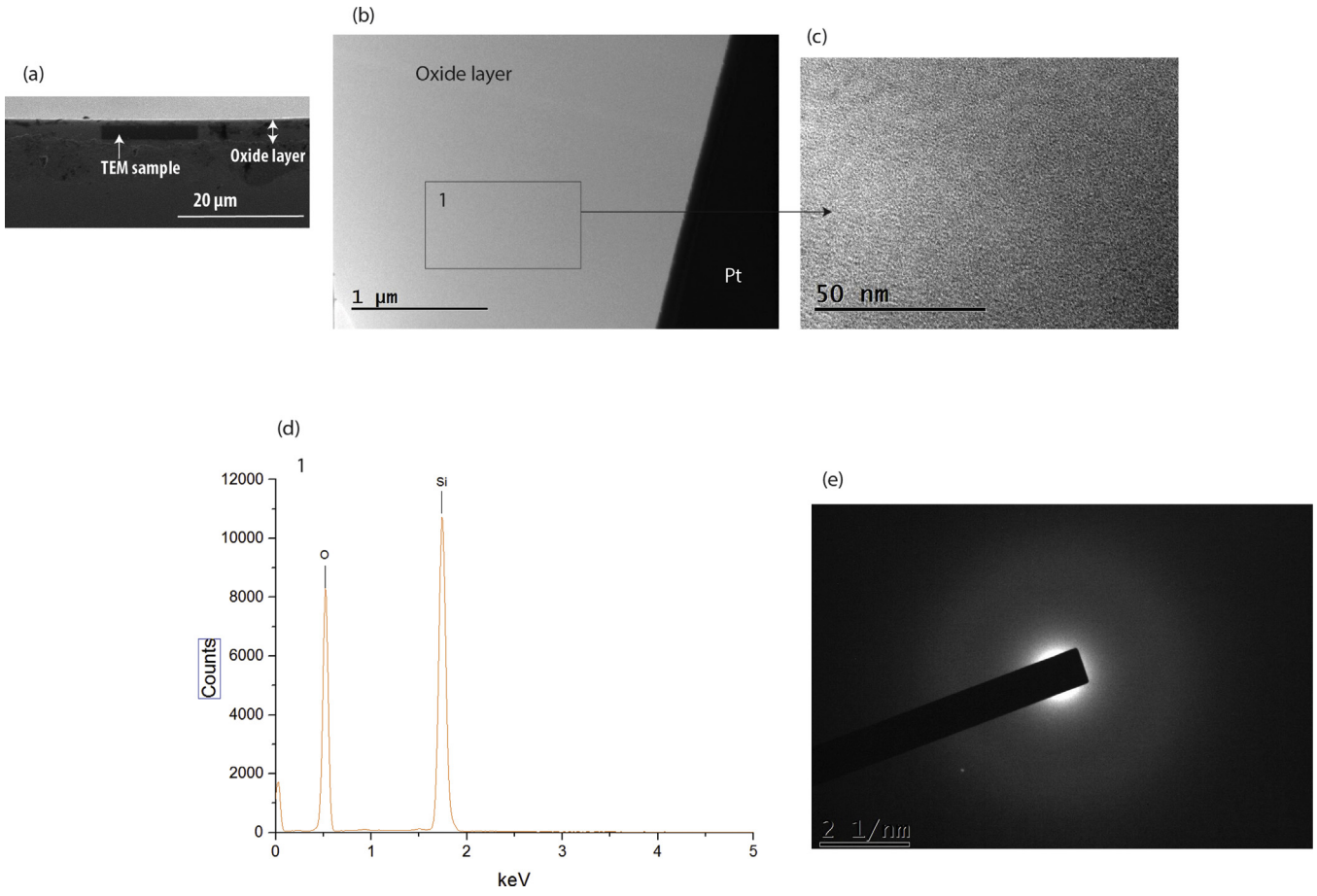

Fig. 9. STEM image of an oxide layer of sample oxidised at 1400 °C for 48 h with corresponding EDS analysis. Diffraction pattern shows that the oxide layer is amorphous.

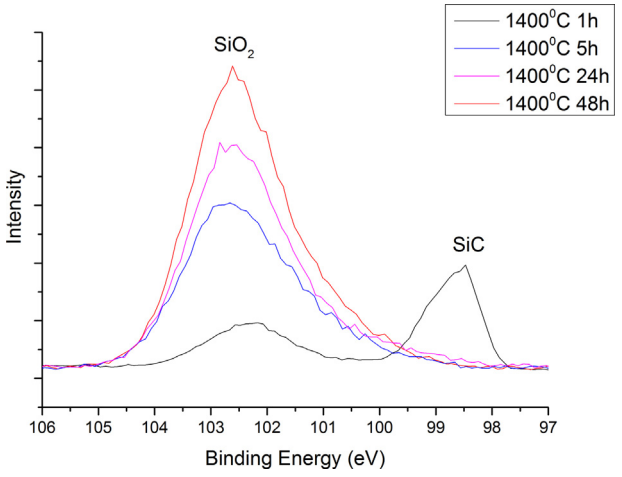

Fig. 10. High resolution Si 2*p* spectra of SiC/SiC CMC samples oxidised at 1400 °C for 1, 5, 24 and 48 h.

behaviour due to oxygen diffusion through the oxide layer. From XRD, EDS and TEM analysis, the oxide layer consists of silicon and oxygen and it has an amorphous structure confirmed by TEM diffraction pattern analysis. The activation energy for oxidation of SiC/SiC composites is 619 kJ mol^{-1} indicating good oxidation resistance compared to monolithic SiC from previous studies where activation energies range from 120 to 480 kJ mol^{-1}. This high activation energy can be explained due to the dense and smooth protective SiO_2 on the outside surface of the CMC passivating and hindering the oxygen penetration. The BN coating was resistant to oxidation after 48 h oxidation at 1400 °C.

Acknowledgments

The authors would like to thank Rolls-Royce plc for providing the financial support for this project. Thanks to the National EPSRC XPS Users' Service (NEXUS) at Newcastle University, an EPSRC Mid-Range Facility for obtaining the X-ray photoelectron spectra.

References

[1] J. Viricelle, P. Goursat, D. Bahloul-Hourlier, Oxidation behaviour of a multi-layered ceramic matrix composite $(SiC)_f/C/(SiBC)_m$, Compos. Sci. Technol. 61 (2001) 607–614.
[2] K. Lee, R. Miller, Oxidation behaviour of mullite-coated SiC and SiC/SiC composites under thermal cycling between room temperature and 1200°–1400 °C, J. Am. Ceram. Soc. 79 (3) (1996) 620–626.
[3] D. Lui, Oxidation of polycrystalline α-silicon carbide ceramics, Ceram. Int. 23 (1997) 425–436.
[4] I. Spitsberg, J. Steibel, Thermal and environmental barrier coatings for SiC/SiC CMCs in aircraft engine applications, Int. J. Appl. Ceram. Technol. 1 (4) (2004) 291–301.
[5] S. Singhal, Oxidation kinetics of hot pressed silicon carbide, J. Mater. Sci. 11 (1976) 1246–1253.
[6] J. Costello, R. Tressler, Oxidation kinetics of silicon carbide crystals and ceramics: I, in dry oxygen, J. Am. Ceram. Soc. 69 (9) (1986) 674–681.
[7] G. Schiroky, Oxidation behaviour of chemically vapor deposited SiC, J. Adv. Ceram. 2 (2) (1987) 137–141.
[8] T. Narushima, T. Goto, T. Hirai, High temperature passive oxidation of chemically vapor deposited silicon carbide, J. Am. Ceram. Soc. 72 (8) (1989) 1386–1390.
[9] E. Sucov, Diffusion of oxygen in vitreous silica, J. Am. Ceram. Soc. 46 (1) (1963) 14–20.

[10] H. Kleykamp, V. Schauer, A. Skokan, Oxidation behaviour of SiC fibre reinforced SiC, J. Nucl. Mater. 227 (1995) 130–137.
[11] B. Sheldon, E. Sun, S. Nutt, J. Brennan, Oxidation of BN-coated SiC fibers in ceramic matrix composites, J. Am. Ceram. Soc. 79 (2) (1996) 539–543.
[12] N. Jacobson, D. Fox, E. Opila, High temperature oxidation of ceramic matrix composites, Pure Appl. Chem. 70 (2) (1998) 493–500.
[13] R. Naslain, SiC-matrix composites: nonbrittle ceramics for thermo-structural application, Int. J. Appl. Ceram. Technol. 2 (2) (2005) 75–84.
[14] B. Deal, A. Grove, General relationshop for the thermal oxidation of silicon, J. Appl. Phys. 36 (12) (1965) 3770–3778.
[15] R.F. Egerton, P. Li, M. Malac, Radiation damage in the TEM and SEM, Micron 35 (2004) 399–409.
[16] G. Ervin, Oxidation behaviour of silicon carbide, J. Am. Ceram. Soc. 41 (9) (1958) 347–352.
[17] W. Pultz, W. Hertl, SiO_2 + SiC reaction at elevated temperatures, Trans. Faraday Soc. 62 (9) (1966) 2499–2504.
[18] C. Ramberg, W. Worrell, Oxgen transport in silica at high temperatures: implications of oxidation kinetics, J. Am. Ceram. Soc. 84 (11) (2001) 2607–2616.
[19] C. Onneby, C. Pantano, Silicon oxycarbides formation on SiC surfaces and at the SiC/SiO_2 interface, J. Vac. Sci. Technol. A 15 (1997) (1597-1062).
[20] W. Pultz, Temperature and oxygen pressure dependence of silicon carbide oxidation, J. Am. Ceram. Soc. 71 (13) (1989) 4556–4558.
[21] L. Ogbuji, E. Opila, A comparison of the oxidation kinetics of SiC and Si_3N_4, J. Electrochem. Soc. 142 (1995) 925–930.
[22] D. Liu, Oxidation of polycrystalline alpha silicon carbide, Ceram. Int. 23 (1997) 425–436.